Journal of Neurochemistry
Lippincott Williams & Wilkins, Inc., Philadelphia

Unique Functional Properties of a Sensory Neuronal P2X ATP-Gated Channel from Zebrafish

Éric Boué-Grabot, *Marie-Andrée Akimenko, and Philippe Séguéla

*Cell Biology of Excitable Tissue Research Group, Department of Neurology and Neurosurgery, Montreal Neurological Institute, McGill University, Montreal, Quebec, and *Loeb Research Institute, Ottawa Hospital, Ottawa, Ontario, Canada*

Abstract: We report here the structural and functional characterization of an ionotropic P2X ATP receptor from the lower vertebrate zebrafish (*Danio rerio*). The full-length cDNA encodes a 410-amino acid-long channel subunit $zP2X_3$, which shares only 54% identity with closest mammalian P2X subunits. When expressed in *Xenopus* oocytes in homomeric form, ATP-gated $zP2X_3$ channels evoked a unique nonselective cationic current with faster rise time, faster kinetics of desensitization, and slower recovery than any other known P2X channel. Interestingly, the order of agonist potency for this P2X receptor was found similar to that of distantly related $P2X_7$ receptors, with benzoylbenzoyl ATP (EC_{50} = 5 μM) $\gg$ ATP (EC_{50} = 350 μM) = ADP > α,β-methylene ATP (EC_{50} = 480 μM). $zP2X_3$ receptors are highly sensitive to blockade by the antagonist trinitrophenyl ATP (IC_{50} < 5 nM) but are weakly sensitive to the noncompetitive antagonist pyridoxal phosphate-6-azophenyl-2′,4′-disulfonic acid. $zP2X_3$ subunit mRNA is exclusively expressed at high levels in trigeminal neurons and Rohon–Beard cells during embryonic development, suggesting that neuronal P2X receptors mediating fast ATP responses were selected early in the vertebrate phylogeny to play an important role in sensory pathways. **Key Words:** Purinoceptor—Nucleotide—Desensitization—Suramin—Sensory neurons—Rohon–Beard cells—*Xenopus* oocytes.
J. Neurochem. **75,** 1600–1607 (2000).

Extracellular ATP released from synaptic vesicles or lytic cells can induce membrane depolarizations through the direct opening of ATP-gated cation channels, or P2X receptors, expressed in a variety of neuronal and non-neuronal populations (North and Barnard, 1997). Despite the short half-life of ATP in the extracellular space (Zimmermann, 1996), the gating of native P2X receptor channels evokes a fast inward current carried by monovalent and calcium ions (Rogers and Dani, 1995; Ueno et al., 1998). Ionotropic purinergic responses have been shown to be involved in a broad range of calcium-dependent signaling events from the neurogenic control of smooth muscle contraction (Burnstock, 1990) to the regulation of neurotransmitter release (MacDermott et al., 1999). The seven genes coding for P2X receptor subunits identified in mammals share 38–48% identity at the protein level. The global architecture of P2X channels with two transmembrane domains, intracellular termini, and a cysteine-rich extracellular loop resembles that of recently discovered proton-gated channels (Waldmann and Ladzunski, 1998). However, no significant homology of primary structure has been observed between P2X and acid-sensing channels. From heterologous expression studies, homomeric P2X channels can be classified in three groups according to their functional and pharmacological properties (for review, see North and Barnard, 1997). The first group of ionotropic ATP receptors with fast desensitization and high sensitivity to the agonists ATP and α,β-methylene ATP ($\alpha\beta$mATP) includes the $P2X_1$ and $P2X_3$ subtypes. They are blocked by nanomolar concentrations of the antagonist 2′-*O*-trinitrophenyl ATP (TNP-ATP) (Virginio et al., 1998). The second group is composed of slowly desensitizing, $\alpha\beta$mATP-insensitive, and suramin-sensitive $P2X_2$ and $P2X_5$ subtypes. The third group contains slowly desensitizing $P2X_4$ and nonneuronal $P2X_7$ subtypes that are also insensitive to $\alpha\beta$mATP and suramin. Recombinant $P2X_6$ homomers have been expressed very rarely in transfected mammalian cells (Collo et al., 1996) and are silent in *Xenopus* oocytes (Soto et al., 1996; Lê et al., 1998). Interestingly, functional heteromeric P2X receptor subtypes resulting from the assembly of $P2X_2$ + $P2X_3$ (Lewis et al., 1995), $P2X_4$ + $P2X_6$ (Lê et al., 1998), or $P2X_1$ + $P2X_5$ (Torres et al., 1998; Lê et al., 1999) subunits display hybrid phenotypes endowed with the pharmacology of the subunit most sensitive to ATP. Despite intensive research on their characterization in heterologous expression systems or in native cells, most key properties of ATP-gated channels are not yet assigned to structural features that could underlie their

Received March 23, 2000; revised manuscript received May 24, 2000; accepted May 26, 2000.

Address correspondence and reprint requests to Dr. P. Séguéla at Montreal Neurological Institute, 3801 University St., Montreal, Quebec, Canada H3A 2B4. E-mail: mips@musica.mcgill.ca

Abbreviations used: $\alpha\beta$mATP, α,β-methylene ATP; bzATP, benzoylbenzoyl ATP; EST, expressed sequence tag; hpf, hours post fertilization; PPADS, pyridoxal phosphate-6-azophenyl-2′,4′-disulfonic acid; TNP-ATP, 2′,3′-*O*-trinitrophenyl ATP.

electrophysiological behavior or their subtype-selective pharmacology. For instance, the residues of the second transmembrane domain lining the hydrophilic pore have been identified by cysteine scan mutagenesis (Rassendren et al., 1997; Egan et al., 1998). Domains of P2X receptors involved in desensitization have been identified (Werner et al., 1996), and a phosphothreonine in an N-terminal protein kinase C site is required for the expression of slowly desensitizing $P2X_2$ channels (Boué-Grabot et al., 2000). Studies on the domains responsible for heteropolymerization have also been published (Torres et al., 1999), but no clear information is available yet on the ATP binding domain, the mechanism of blockade by suramin and other noncompetitive antagonists, or the determinants of the weak selectivity of P2X cation channels for small cations. Thus, functional comparisons between mammalian P2X subunits and P2X subunits from distant lower species would likely be helpful to investigate the specific structure–activity relationships of this class of excitatory neurotransmitter-gated channels, unrelated in sequence and transmembrane topology to nicotinic acetylcholine or glutamate receptor channels. We report here the primary structure and electrophysiological and pharmacological properties of an ionotropic ATP receptor expressed in the nervous system of the lower vertebrate zebrafish *Danio rerio.* This member of the P2X gene family is the most phylogenetically distant from the mammalian subunits known so far and defines by itself a novel phenotypic group of nucleotide-gated channels.

EXPERIMENTAL PROCEDURES

Molecular cloning and in situ hybridization

Using the program tblastn (Altschul et al., 1990) to search the GenBank database with a virtual probe corresponding to a consensus P2X channel subunit, a novel partial P2X sequence was identified in the nucleotide sequence AI588766 from the Washington University zebrafish EST (Expressed Sequence Tag) project. The full-length zebrafish P2X clone ($zP2X_3$) corresponding to the EST was isolated from a directional oligo dT-primed cDNA library constructed from various pooled embryonic stages and adult liver, and complete automatic sequencing was performed on both strands. In situ hybridization was carried out on whole-mount preparations of embryos at various stages with 1.4-kb full-length antisense riboprobes labeled with digoxygenin, as previously described by Thisse et al. (1993).

Injection of oocytes with recombinant channels

Original clone in pSport1 vector was transferred into pCDNA3 vector (Invitrogen) with cytomegalovirus promoter for expression in oocytes. Ovary lobes were surgically retrieved from *Xenopus laevis* frogs under deep Tricaine (Sigma) anesthesia. Oocyte-positive lobes were then treated for 3 h at room temperature with type I collagenase (Life Technologies) in calcium-free Barth's solution under vigorous agitations. Stage V–VI oocytes were then manually defolliculated before nuclear microinjections of 5 ng of supercoiled plasmid coding for $zP2X_3$, rat $P2X_3$, or rat $P2X_1$ subunit. The cells were maintained in Barth's solution containing 1.8 m*M* calcium chloride and 10 μg/ml gentamicin (Sigma) at 19°C for up to 5 days.

Electrophysiology and data analysis

Two-electrode voltage-clamp recordings were made 1–3 days after microinjection using an OC-725B amplifier (Warner Instruments). Cells were voltage clamped at −60 mV. Signals were low-pass filtered at 1 kHz, acquired at 500 Hz using a Macintosh IIci computer equipped with an NB-MIO-16XL analog-to-digital interface (National Instruments). Recorded traces were postfiltered at 20–50 Hz in Axograph (Axon Instruments) for purpose of illustration only. Ringer's solution containing 115 m*M* NaCl, 2.5 m*M* KCl, 1.8 m*M* $CaCl_2$, and 10 m*M* HEPES buffered at pH 7.4 was perfused onto oocytes at a constant flow rate of 10–12 ml/min. The volume of the bath in the perfusion chamber was set to 200–250 μl. Agonists ATP, benzoylbenzoyl ATP (bzATP), $\alpha\beta$mATP, and ADP and antagonists suramin, pyridoxal phosphate-6-azophenyl-2′,4′-disulfonic acid (PPADS), and 2′,3′-*O*-trinitrophenyl ATP (TNP-ATP; Sigma) were prepared in bath perfusion buffer at their final concentration. Dose–responses curves and kinetic analysis were carried out using the Prism 2.0 software (GraphPad, San Diego, CA, U.S.A.). Agonist concentration–response curves, EC_{50} values, and cooperativity indexes were derived from fittings to the Hill sigmoidal equation. Activation and desensitization curves were fitted with monoexponential growth and monoexponential decay equations, respectively. Time constants for 50% activation and 50% desensitization were then derived to quantitate the differences of kinetic properties between $zP2X_3$, rat $P2X_1$, and rat $P2X_3$ receptors.

RESULTS

Primary structure of $zP2X_3$ receptor subunit

A novel partial P2X subunit was identified by BLAST (Basic Local Alignment Search Tool) in the EST AI588766 located in the 3′ region of a zebrafish mRNA. The 1,462-nucleotide-long full-length cDNA clone corresponding to this EST encodes a membrane protein with the characteristic pattern of features of a P2X ATP-gated channel subunit (Fig. 1). At the nucleotide level, this cDNA displays 59% identity with rat $P2X_3$ in the coding region. The predicted protein of 410 amino acids has 54% identity with rat $P2X_3$, 41% with rat $P2X_2$, 33–39% with rat $P2X_1$, $P2X_4$, $P2X_5$, or $P2X_6$, and 32% with the nonneuronal rat $P2X_7$. On this structural basis, we decided to name this subunit $zP2X_3$, despite significant functional differences with rat $P2X_3$ (see below). Hydrophobicity analysis and alignment with known P2X subunits predicted an intracellular N-terminal domain of 33 amino acids, a first transmembrane domain of 18 amino acids, an extracellular loop of 280 amino acids with the 10 conserved cysteines characteristic of the P2X receptor family, and a second transmembrane domain of 26 amino acids followed by a C-terminal domain of 53 amino acids (Fig. 1).

Functional characterization of homomeric $zP2X_3$ channels

When expressed in *Xenopus* oocytes, $zP2X_3$ subunits assembled in homomeric ATP-gated channels (Fig. 2). A fast inward current of 0.44 ± 0.1 μA (n = 8) was evoked by applications of 100 μM extracellular ATP, followed by fast desensitization of the channels during the application of the agonist (Fig. 2A). From its reversal potential close to 0 mV (E_{rev} = +5 mV) measured from

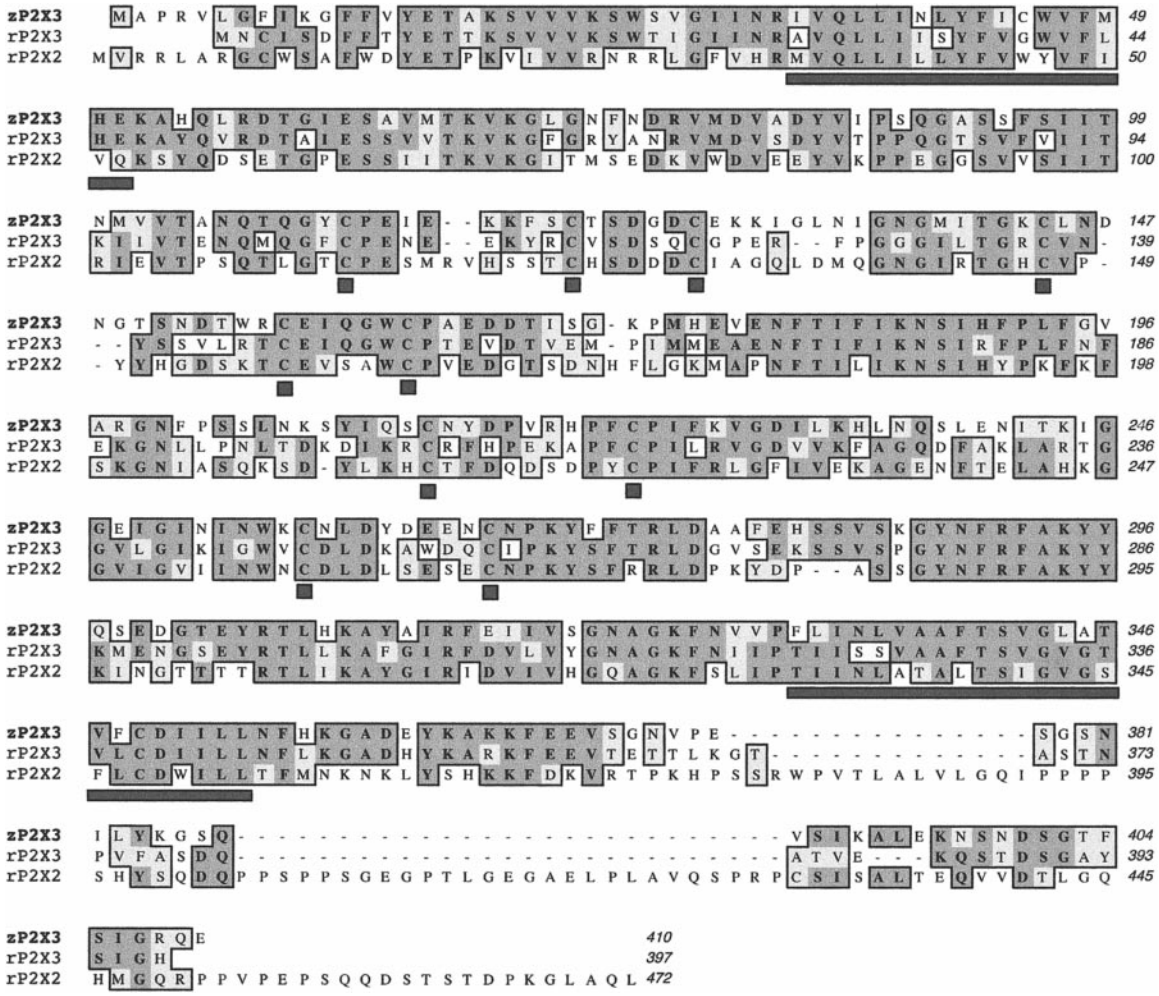

FIG. 1. Primary structure of zP2X$_3$ subunit and alignment with closest mammalian P2X ATP-gated channel subunits, rat P2X$_3$ and rat P2X$_2$. The two predicted transmembrane domains are underlined, and the 10 extracellular cysteines conserved in all known P2X subunits are indicated by dark squares. Nucleotide and protein sequences of zP2X$_3$ subunit have been deposited in the GenBank database (accession no. AF237683).

current–voltage relationship plots, we concluded that the zP2X$_3$-mediated inward current is carried by cations and that the zP2X$_3$ ATP-gated channels are nonselective cation channels (Fig. 2B). No inward or outward rectification was observed between −60 and +60 mV, indicating the absence of a voltage-dependent mechanism in the operation of these channels in this range of membrane potentials. Likely related to their fast kinetics of desensitization, the zP2X$_3$ receptors never recovered their full response to ATP from the first stimulation, even after several minutes of agonist washout (Fig. 2C). We observed and reported this property of partial recovery with homomeric P2X$_1$ receptors (Lê et al., 1999). On the contrary, rat P2X$_3$ receptors recovered completely after 3–5 min in the same conditions (Fig. 2C).

The zP2X$_3$ ATP receptors responded to extracellular nucleotides with unusually fast kinetics (Figs. 2 and 3). To quantitatively compare several fast P2X phenotypes recorded in the same heterologous expression system with the same protocol of agonist application (see inset in Fig. 3), we measured the time constant for half-activation (τa_{50}) of rat P2X$_1$, rat P2X$_3$, and zP2X$_3$ by fitting the relation between time before peak and percentage of peak response. The single exponential fitting gave a $\tau a_{50} = 20 \pm 5$ ms for zP2X$_3$ compared with a $\tau a_{50} = 225$–230 ± 60 ms for both rat P2X$_1$ and P2X$_3$ receptors (Fig. 3A). Even taking into account the experimental underestimation of the time necessary to reach the peak current due to fast desensitization, these values emphasized the unique speed of activation of zP2X$_3$ channels at the whole-cell level. Using a similar approach, we compared the kinetics of desensitization of zP2X$_3$ with rat P2X$_1$ and rat P2X$_3$. Again, zP2X$_3$ channels were found to be the fastest of all known P2X subtypes, with a time constant of desensitization of 40 ± 18 ms compared with 374 ± 55 and 665 ± 75 ms for rat P2X$_1$ and P2X$_3$, respectively.

We tested the potency of several agonists to activate zP2X$_3$ receptors (Fig. 4). The response to large concentra-

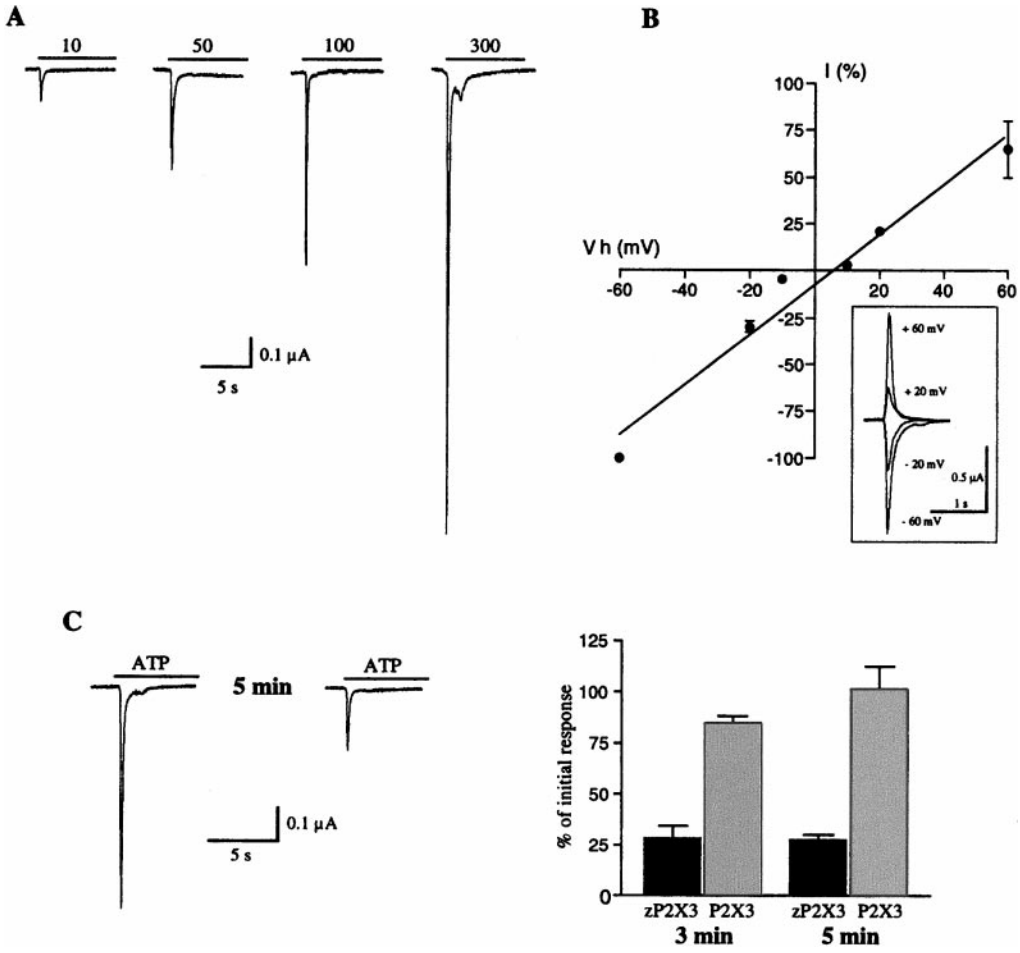

FIG. 2. Representative fast phenotype of ATP-induced currents mediated by homomeric $zP2X_3$ nonselective cation channels. **A:** Typical currents recorded from oocytes expressing $zP2X_3$ in response to different concentrations of ATP indicated in micromolar at the top of each trace. **B:** Current–voltage relationship of homomeric $zP2X_3$ ATP-gated channels. Peak currents (means ± SEM from 7–11 oocytes) recorded at different holding membrane potentials (illustrated in **inset**) were normalized to the maximal responses obtained at −60 mV. **C:** Partial recovery after 5-min washings between ATP applications and comparison with rat $P2X_3$ phenotype.

tions (≥500 μM) of ATP or $\alpha\beta$mATP did not reach a maximum, so their EC_{50} values are only conservative estimations. However, the kinetics of currents evoked by equieffective doses of the different agonists were similar (see inset in Fig. 4A), as were the slopes of their activation curves (Fig. 4A). ATP (EC_{50} = 350 ± 57 μM) was found to be much less potent than bzATP (EC_{50} = 5 ± 1 μM), equipotent to ADP (EC_{50} = 322 ± 77 μM), but significantly more potent than $\alpha\beta$mATP (EC_{50} = 479 ± 22 μM) to gate the $zP2X_3$ channels. The index of cooperativity of the dose–response curve for bzATP was n_H = 2.2. We tested also the sensitivity of $rP2X_3$ to bzATP and measured an EC_{50} of 8 ± 1 μM (data not shown). Differences in the profile of sensitivity to the agonists bzATP, ATP, $\alpha\beta$mATP, and ADP between zebrafish and rat $P2X_3$ receptors are represented in Fig. 4B.

The antagonist TNP-ATP blocks $P2X_1$- and $P2X_3$-containing receptors with high affinity (Virginio et al., 1998; Lê et al., 1999). We show here that TNP-ATP also inhibits $zP2X_3$ channels at nanomolar concentrations, when co-applied with ATP after preincubation: 5 nM TNP-ATP suppressed 80% of the maximal response to 300 μM ATP (Fig. 5). The antagonist suramin spared 25% of the maximal response to ATP when applied at 40 μM. However, contrasting with the mammalian $P2X_3$ receptors, >20% of maximal ATP-gated currents remained after application of 30 μM PPADS in the same conditions, and a significant current was still recorded at 100 μM (Fig. 5). By comparison, rat $P2X_3$ receptors are completely blocked by 30 μM PPADS, with an IC_{50} = 1.5 μM (Lewis et al., 1995).

Cellular distribution of $zP2X_3$ mRNA during development

Anatomical localization of $zP2X_3$ transcripts using in situ hybridization revealed that these ATP-gated channel subunits are exclusively expressed in the nervous system during development (Fig. 6A). Only two subsets of central neurons transcribe $zP2X_3$ gene in the embryo during the stage corresponding to 24–48 h post fertilization

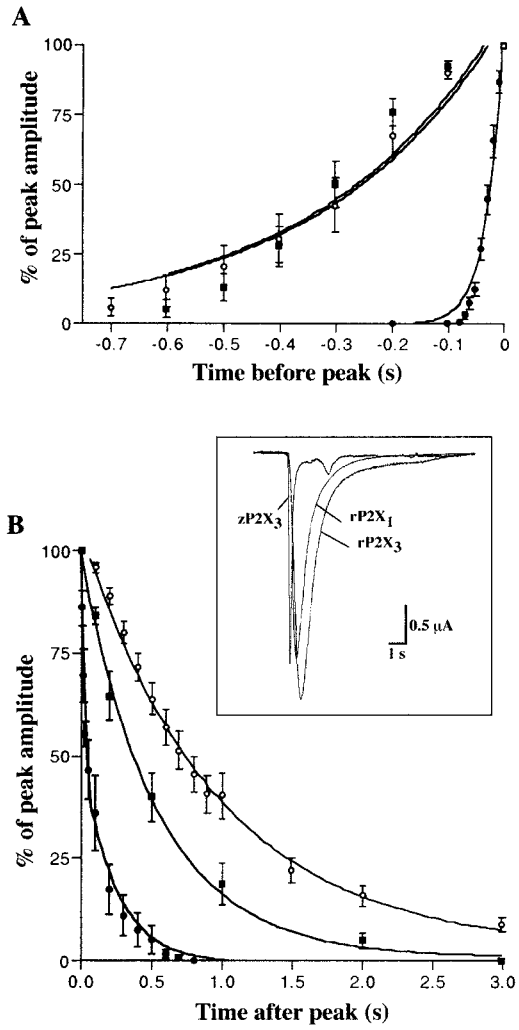

FIG. 3. $zP2X_3$ channels display fastest kinetics of activation and desensitization in P2X family. Shown is a comparison of the rates of activation (**A**) and desensitization (**B**) of $zP2X_3$ (filled circles) with rat $P2X_1$ (filled squares) and rat $P2X_3$ (open circles). We measured at different times before and after the peak the response evoked by application of 300 μM ATP for $zP2X_3$ (n = 10) and 50 μM ATP for rat $P2X_1$ (n = 7) and rat $P2X_3$ (n = 7). **Inset:** Superimposed traces of representative ATP-induced currents obtained in *Xenopus* oocytes injected with $zP2X_3$, $rP2X_1$, and $rP2X_3$.

(hpf): the neurons from the trigeminal ganglia in the rhombencephalon (Fig. 6A and B) and the Rohon–Beard cells in the spinal cord (Fig. 6A and C). These two populations of neurons are primary sensory neurons. From their common set of genetic (Korzh et al., 1993; Martin et al., 1998) and immunocytochemical (Metcalfe et al., 1990; Canger et al., 1998) markers, trigeminal and Rohon–Beard neurons seem to share the same development program despite their different localization. Furthermore, both types of neurons are among the earliest neurons to send axons (Canger et al., 1998) and are mechanosensory neurons that participate in the motor responses to touch, the first behavioral response of the embryo (Bayer and Campos-Ortega, 1992). We noticed that the expression of $zP2X_3$ is regulated during development: Neuronal $zP2X_3$ expression peaks at 24–48 hpf and then disappears completely from spinal cord at 72 hpf. Rohon–Beard cells die before the adult stage when they are functionally replaced by peripheral dorsal root ganglia (Ribera and Nusslein-Vohlard, 1998), so the expression of $zP2X_3$ seems to follow the fate of these transient spinal sensory neurons. A small number of positive neurons remained detectable in trigeminal nuclei at 96 hpf. Using RT-PCR, we detected $zP2X_3$ mRNA in the adult animal (data not shown), where $zP2X_3$ channels might participate in the excitability of peripheral trigeminal and dorsal root ganglion neurons (Cook et al., 1997).

DISCUSSION

The predicted structure of $zP2X_3$, a novel member of the P2X ATP receptor family, displays all the key elements that characterize these channels activated by extracellular nucleotides. The N-terminal domain of $zP2X_3$ contains the highly conserved protein kinase C phosphorylation site with the acceptor Thr^{17} that has recently been shown to control the kinetic properties of $P2X_2$ channel subtype (Boué-Grabot et al., 2000). Seven Asn-glycosylation consensus sites have been counted in the extracellular domain of $zP2X_3$, but the potential acceptor Asn^{180} is the only one at the same relative position in rat $P2X_3$ and in other subunits. A protein kinase C site is also present in the C-terminal domain of $zP2X_3$. This potential site of phosphorylation could have an impact on the activity of $zP2X_3$ channels because a protein kinase A site located in the C-terminal domain of $P2X_2$ has been reported to be involved in the modulation of desensitization (Chow and Wang, 1998). Interestingly, the motif EKXSXDSGX(Y/F)SIG is found in the distal part of the C-terminal domain of human (Garcia-Guzman et al., 1997), rat (Chen et al., 1995; Lewis et al., 1995), mouse (Souslova et al., 1997), and zebrafish $P2X_3$ subunits. The presence of this conserved stretch of amino acids in vertebrate $P2X_3$ subunits suggests that it could play a role in intrasubunit interactions, in a $P2X_3$-specific mechanism of heteromeric assembly, or in the association of $P2X_3$ subunits with a conserved heterologous intracellular partner.

Despite significant homology with rat $P2X_3$ at the protein level, we noticed some unique aspects of the function of homomeric $zP2X_3$ channels during their electrophysiological characterization in *Xenopus* oocytes. The small difference of EC_{50} for bzATP between rat and zebrafish $P2X_3$ was found not significant (Fig. 4B), and ADP has also a similar potency for zebrafish and rat $P2X_3$ (Chen et al., 1995; Lewis et al., 1995). However, we observed that ATP and $\alpha\beta$mATP, two high-affinity agonists for the mammalian $P2X_1$ and $P2X_3$ receptors (Valera et al., 1994; Chen et al., 1995; Lewis et al., 1995), have a much lower potency (<200 times) for $zP2X_3$. These major differences with the pharmacological profile of rat $P2X_3$ demonstrated that the primary

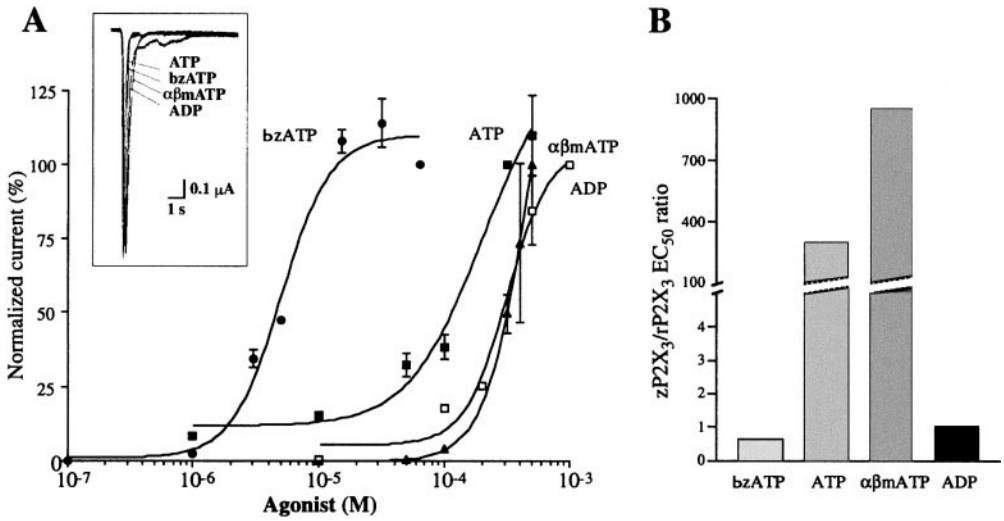

FIG. 4. Sensitivity of $zP2X_3$ receptors to the agonists ATP, ADP, bzATP, and $\alpha\beta$mATP. **A:** Dose–response curves for the agonists ATP (filled squares), ADP (open squares), bzATP (filled circles), and $\alpha\beta$mATP (filled triangles). Mean peak currents were normalized to the maximal response for bzATP, to the response obtained with 300 μM for ATP, with 500 μM for $\alpha\beta$mATP, and with 800 μM for ADP. Each point corresponds to the average of data obtained from 8–12 oocytes. **Inset:** Similar desensitization kinetics of the response of $zP2X_3$ channels to different agonists. **B:** Comparison of agonist sensitivity between $zP2X_3$ and rat $P2X_3$. EC_{50} values of ATP, $\alpha\beta$mATP, and ADP for rat $P2X_3$ were obtained from Chen et al. (1995) and Lewis et al. (1995).

structure of a novel P2X channel subunit is not currently a reliable predictor of its pharmacology. Indeed, the rank order of agonist potency for $zP2X_3$ was closest to the one of more distantly related nonneuronal $P2X_7$ receptor that is more sensitive to bzATP than to ATP in recombinant (Surprenant et al., 1996) or native (Steinberg et al., 1987) forms in macrophages.

The homomeric $zP2X_3$ channels thus define a novel phenotype for ATP-gated channels with fast kinetics of desensitization, with bzATP being a more potent agonist than ATP and with a weak sensitivity to PPADS. Constructions of functional chimeras containing domains of mammalian and zebrafish $P2X_3$ subunits should facilitate the identification of regions involved in sensitivity to agonists, in high-affinity blockade by noncompetitive antagonists, or in recovery from desensitization. We believe that the partial but significant homology between the extracellular domains of rat $P2X_3$ and $zP2X_3$ subunits (56%) will increase the chance of getting functional chimeric receptors with informative pharmacology. A chimera with the transmembrane domains and intracellular termini of $zP2X_3$ and a part of or the whole extracellular domain of rat $P2X_3$ would be helpful to pinpoint the structural elements conferring the high sensitivity to ATP and $\alpha\beta$mATP as well as the determinants of high sensitivity to blockade by PPADS.

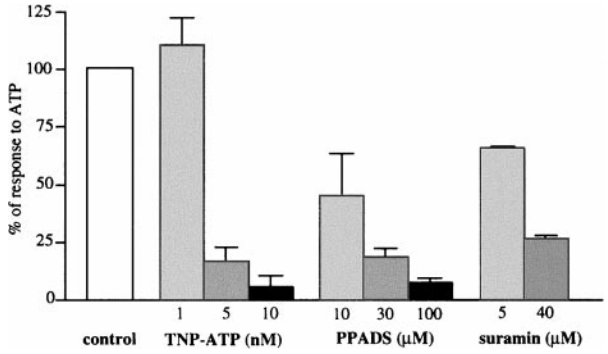

FIG. 5. Differential blockade of $zP2X_3$ activation by the antagonists TNP-ATP, PPADS, and suramin. Amplitude of responses (means ± SEM, n = 6–11) to co-application of 300 μM ATP is shown with different concentrations of antagonist as a percentage of the response to ATP alone (control response). In all cases, oocytes were preincubated during 30 s with the antagonist alone.

All known neuronal P2X receptor subunits are expressed in peripheral sensory ganglia in mammals (Collo et al., 1996). From our in situ hybridization results, the expression of $zP2X_3$ restricted to primary sensory neurons appears to mirror the sensory-specific anatomical localization of rodent $P2X_3$ subunits (Chen et al., 1995). Such a conserved pattern of cellular expression suggests strongly that the $P2X_3$ subunit/subtype of ATP receptors has been selected early during vertebrate phylogeny, and likely before the vertebrates arose, for the detection of sensory inputs. The fast kinetics of activation and desensitization of zebrafish and mammalian $P2X_3$ channels could have been one of the main physiological properties maintained in vertebrates by selective pressure. The high sensitivity to ATP of mammalian $P2X_3$, not found in zebrafish receptors, would then correspond to a more recent functional acquisition. The low sensitivity of $zP2X_3$ receptors to the endogenous agonist candidate ATP could indicate also that other ligands activate them more efficiently or that co-agonists are required. Several

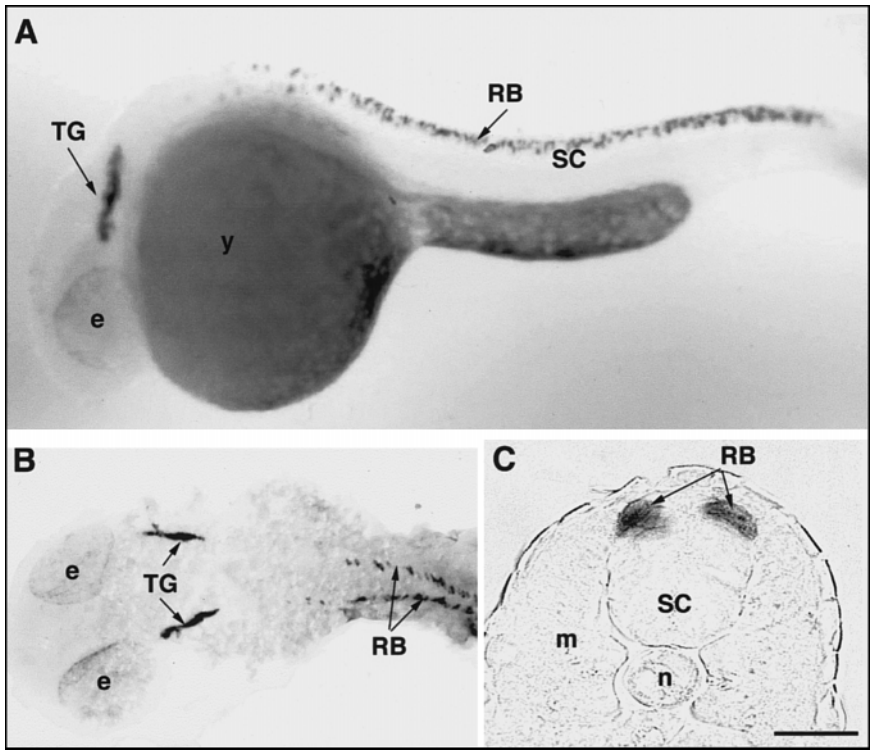

FIG. 6. Neuronal localization of $zP2X_3$ gene expression in zebrafish embryo. **A:** Cells in the trigeminal ganglia (TG) and Rohon–Beard neurons (RB) in the spinal cord (SC) express high levels of $zP2X_3$ transcripts at 24 hpf. **B:** Dorsal view of a 24 hpf embryo with the yolk sac dissected out. Characteristic bilateral rows of $zP2X_3$-expressing neurons are labeled in the trigeminal ganglia and Rohon–Beard cells. **C:** Transverse section through the trunk of an embryo of the same stage as in A, showing $zP2X_3$-positive Rohon–Beard neurons located in the dorsal horn of spinal cord. Bar = 130 μm (A and B) and 30 μm (C). e, eyes; n, notochord; m, trunk muscle; y, yolk sac.

neuronal P2X subtypes are sensitive to extracellular protons and zinc ions (Cook et al., 1997; Stoop et al., 1997), so we tested the effects of co-application of alkaline (pH 8.5) and acidic (pH 6.3) solutions and 50 μM zinc chloride ions with 100 μM ATP on $zP2X_3$, but we did not record any significant difference with ATP alone (data not shown). In a subset of rodent small-diameter sensory neurons, $P2X_3$ subunits associate with $P2X_2$ to generate functional $P2X_{2+3}$ receptors with hybrid properties; thus, it is probable that $zP2X_3$ subunits assemble natively with other P2X partners during development and in the adult. Other P2X genes expressed in trigeminal and Rohon–Beard sensory neurons of zebrafish remain to be identified and cloned to test subunit combinations and investigate how $zP2X_3$ contributes to the phenotype of heteromeric channels. Thanks to a short life cycle in autonomous stages, the zebrafish has been chosen as a particularly good experimental model to dissect the role of specific genes in vertebrate development. With use of dominant negative transgenes or antisense technology, it will be interesting to study the impact of a knockout of the functional expression of $zP2X_3$ subunits during development to increase our understanding of the role of ATP-gated channels in sensory transmission in lower vertebrates and in mammals.

Acknowledgment: The authors thank Audrey Speelman and Lynda Laforest for their expert technical assistance as well as Mark Ekker (Loeb Research Institute, Ottawa) for helpful comments and advice. This work has been supported by the Medical Research Council of Canada, the Heart and Stroke Foundation of Canada, and AstraZeneca Charnwood. Éric Boué-Grabot is a postdoctoral fellow of the Savoy Foundation for Epilepsy, and Philippe Séguéla is a senior Scholar of the Fonds de la Recherche en Santé du Québec.

REFERENCES

Altschul S. F., Gish W., Miller W., Myers E. W., and Lipman D. J. (1990) Basic local alignment search tool. *J. Mol. Biol.* **215,** 403–410.

Bayer T. A. and Campos-Ortega J. A. (1992) A transgene containing lacZ is expressed in primary sensory neurons in zebrafish. *Development* **115,** 421–426.

Boué-Grabot E., Archambault V., and Séguéla P. (2000) A protein kinase C site highly conserved in P2X subunits controls the desensitization kinetics of P2X2 ATP-gated channels. *J. Biol. Chem.* **275,** 10190–10195.

Burnstock G. (1990) Dual control of local blood flow by purines. *Ann. NY Acad. Sci.* **603,** 31–45.

Canger A. K., Passini M. A., Asch W. S., Leake D., Zafonte B. T., Glasgow E., and Schechter N. (1998) Restricted expression of the neuronal intermediate filament protein plasticin during zebrafish development. *J. Comp. Neurol.* **399,** 561–572.

Chen C.-C., Akopian A. N., Sivilotti L., Colquhoun D., Burnstock G., and Wood J. N. (1995) A P2X purinoceptor expressed by a subset of sensory neurons. *Nature* **377,** 428–431.

Chow Y.-W. and Wang H.-L. (1998) Functional modulation of P_{2X2} receptors by cyclic AMP-dependent protein kinase. *J. Neurochem.* **70,** 2606–2612.

Collo G., North R. A., Kawashima E., Merlo-Pich E., Neidhart S., Surprenant A., and Buell G. (1996) Cloning of P2X5 and P2X6 receptors and the distribution and properties of an extended family of ATP-gated ion channels. *J. Neurosci.* **16,** 2495–2507.

Cook S. P., Vulchanova L., Hargreaves K. M., Elde R., and McClesky E. W. (1997) Distinct ATP receptors mediate ATP actions on nociceptive and non-nociceptive neurons. *Nature* **387,** 505–508.

Egan T. M., Haines W. R., and Voigt M. M. (1998) A domain contributing to the ion channel of ATP-gated P2X2 receptors identified by the substituted cysteine accessibility method. *J. Neurosci.* **18,** 2350–2359.

Garcia-Guzman M., Stuhmer W., and Soto F. (1997) Molecular characterization and pharmacological properties of the human P2X3 purinoceptors. *Mol. Brain Res.* **47,** 59–66.

Korzh V., Edlund T., and Thor S. (1993) Zebrafish primary neurons initiate expression of the LIM homeodomain protein Isl-1 at the end of gastrulation. *Development* **118,** 417–425.

Lê K.-T., Babinski K., and Séguéla P. (1998) Central P2X4 and P2X6 channel subunits coassemble into a novel heteromeric ATP receptor. *J. Neurosci.* **18,** 7152–7159.

Lê K. T., Boué-Grabot E., Archambault V., and Séguéla P. (1999) Functional and biochemical evidence for heteromeric ATP-gated channels composed of P2X1 and P2X5 subunits. *J. Biol. Chem.* **274,** 15415–15419.

Lewis C., Neidhart S., Holy C., North R. A., Buell G., and Surprenant A. (1995) Coexpression of P2X2 and P2X3 receptor subunits can account for ATP-gated currents in sensory neurons. *Nature* **377,** 432–435.

MacDermott A. B., Role L. W., and Siegelbaum S. A. (1999) Presynaptic ionotropic receptors and the control of transmitter release. *Annu. Rev. Neurosci.* **22,** 443–485.

Martin S. C., Sandell J. H., and Heinrich G. (1998) Zebrafish TrkC1 and TrkC2 receptors define two different cell populations in the nervous system during the period of axonogenesis. *Dev. Biol.* **195,** 114–130.

Metcalfe W. K., Myers P. Z., Trevarrow B., Bass M. B., and Kimmel C. B. (1990) Primary neurons that express the L2/HNK-1 carbohydrate during early development in the zebrafish. *Development* **110,** 491–504.

Nakazawa K. and Ohno Y. (1997) Effects of neuroamines and divalent cations on cloned and mutated ATP-gated channels. *Eur. J. Pharmacol.* **325,** 101–108.

North R. A. and Barnard E. A. (1997) Nucleotide receptors. *Curr. Opin. Neurobiol.* **7,** 346–357.

Rassendren F., Buell G., Newbolt A., North R. A., and Surprenant A. (1997) Identification of amino acid residues contributing to the pore of a P2X receptor. *EMBO J.* **16,** 3446–3454.

Ribera A. B. and Nusslein-Volhard C. (1998) Zebrafish touch-insensitive mutants reveal an essential role for the developmental regulation of sodium current. *J. Neurosci.* **18,** 9181–9191.

Rogers M. and Dani J. A. (1995) Comparison of quantitative calcium flux through NMDA, ATP, and ACh receptor channels. *Biophys. J.* **68,** 501–506.

Soto F., Garcia-Guzman M., Karschin C., and Stuhmer W. (1996) Cloning and tissue distribution of a novel P2X receptor from rat brain. *Biochem. Biophys. Res. Commun.* **223,** 456–460.

Souslova V., Ravenall S., Fox M., Wells D., Wood J. N., and Akopian A. N. (1997) Structure and chromosomal mapping of the mouse $P2X_3$ gene. *Gene* **195,** 101–111.

Steinberg T. H., Newman A. S., Swanson J. A., and Silverstein S. C. (1987) ATP^{4-} permeabilizes the plasma membrane of mouse macrophages to fluorescent dyes. *J. Biol. Chem.* **262,** 8884–8888.

Stoop R., Surprenant A., and North A. (1997) Different sensitivities to pH of ATP-induced currents at four cloned P2X receptors. *J. Neurophysiol.* **78,** 1837–1840.

Surprenant A., Rassendren F., Kawashima E., North R. A., and Buell G. (1996) The cytolytic P2Z receptor for extracellular ATP identified as a P2X receptor (P2X7). *Science* **272,** 735–738.

Thisse C., Thisse B., Schilling T. F., and Postlethwait J. H. (1993) Structure of the zebrafish snail1 gene and its expression in wild-type, spadetail, and no tail mutant embryos. *Development* **119,** 1203–1215.

Torres G. E., Haines W. R., Egan T. M., and Voigt M. M. (1998) Co-expression of P2X1 and P2X5 receptor subunits reveals a novel ATP-gated ion channel. *Mol. Pharmacol.* **54,** 989–993.

Torres G. E., Egan T. M., and Voigt M. M. (1999) Identification of a domain involved in ATP-gated ionotropic receptor subunit assembly. *J. Biol. Chem.* **274,** 22359–22365.

Ueno S., Koizumi S., and Inoue K. (1998) Characterization of Ca^{2+} influx through recombinant P2X receptor in C6BU-1 cells. *Br. J. Pharmacol.* **124,** 1484–1490.

Valera S., Hussy N., Evans R. J., Adami N., North R. A., Surprenant A., and Buell G. (1994) A new class of ligand-gated ion channel defined by P2X receptor for extracellular ATP. *Nature* **371,** 516–519.

Virginio C., Robertson G., Surprenant A., and North A. (1998) Trinitrophenyl-substituted nucleotides are potent antagonists selective for P2X1, P2X3 and heteromeric P2X2/3 receptors. *Mol. Pharmacol.* **53,** 969–973.

Waldmann R. and Ladzunski M. (1998) H^+-gated cation channels: neuronal acid sensors in the NaC/DEG family of ion channels. *Curr. Opin. Neurobiol.* **8,** 418–424.

Werner P., Sewakdi E. P., Buell G. N., and North R. A. (1996) Domains of P2X receptors involved in desensitization. *Proc. Natl. Acad. Sci. USA* **93,** 15485–15490.

Zimmermann H. (1996) Biochemistry, localization and functional roles of ecto-nucleotidases in the nervous system. *Prog. Neurobiol.* **49,** 589–618.